Comparative Seismic Noise on the Ocean Bottom and on Land

HUGH BRADNER AND JAMES G. DODDS

Institute of Geophysics and Planetary Physics
University of California at San Diego, La Jolla

Abstract. Recordings of the seismic noise background have been made on the Pacific Ocean bottom at a depth of 5 km with internally recording single-component and three-component seismometers which are recovered after automatic release of ballast. Simultaneous recordings have been made at land stations. High-resolution noise spectra in the frequency band between 0.12 and 9 cps have been obtained by digital analysis. Comparison of amplitudes or phase shifts does not indicate coherence between two distant records, and relative energy distribution between orthogonal components of a three-component seismometer record does not indicate significant Rayleigh wave energy. The ocean-bottom noise spectrum has a shape qualitatively similar to the continental land noise spectrum, but greater in magnitude. The Hawaiian Island spectra show the usual 6- to 8-sec microseism peak, but less high-frequency structure than the continental United States spectra.

Introduction. This paper deals with the simultaneous measurements of microseism background spectra on the deep ocean bottom and on land, during the winter and spring 1963. Our data are in the range $1/8$ to 9 cps, limited on the lower end by the response of the seismometer and on the upper end by high cutoff filters in the amplifier. The $1/4$- to $1/8$-cps microseism peak is of particular interest because of the conflicting theories about its origin.

Measurements on land have shown that the bulk of the directional energy is in the form of Rayleigh waves [*Monakhov and Dolbilkina,* 1958, 1960; *Haubrich and Iyer,* 1962]. There is abundant evidence that the microseism peak is associated with large storms at sea [see for example *Donn,* 1954]. On the other hand, some observers have felt that microseism storms can be generated by waves pounding the shore. A recent experiment gives very good evidence that a microseism peak can be generated by the standing waves that occur in a zone a few hundred kilometers wide when ocean swells reflect from the shore [*Haubrich et al.,* 1963].

Ocean bottom microseisms far from shore should be stronger than continental microseisms if they are generated by oceanic storms. Conversely, if generated on land, microseisms should be weaker on the ocean bottom. Relative intensities associated with near-shore generation will depend on the attenuation of the waves in moving from ocean to land.

A three-component instrument can indicate the direction of Rayleigh energy flow. Also, some information on the refraction across the ocean-continent interface might be obtained by comparing ocean and land records.

Apparatus. The ocean-bottom measurements are made with a modified version of the lunar seismometer that was developed at the California Institute of Technology Jet Propulsion Laboratory [*Lehner,* 1962]. The instrument package, consisting of the seismometer and its associated electronics, in a spherical aluminum pressure vessel, is buoyant. A lead weight in the form of a spike is rigidly attached to the package to make it sink and to effect coupling to the ocean bottom. When recording is completed, the lead anchor is detached from the instrument, which then floats to the surface. To facilitate retrieval of the instrument, a radio transmitter turns on when the sphere reaches the surface. There is no link between the instrument and the surface during the recording.

This paper deals with records from an ocean-bottom single-component vertical seismograph, an ocean-bottom 3-component equiangular seismograph, and a dry-land single-component vertical seismograph. Each package is a self-contained recording seismometer. The signal from an electromagnetic seismometer is amplified, passed through a voltage-to-frequency modulator, and recorded on magnetic tape. Precision tuning-fork timing circuits turn on the amplifier

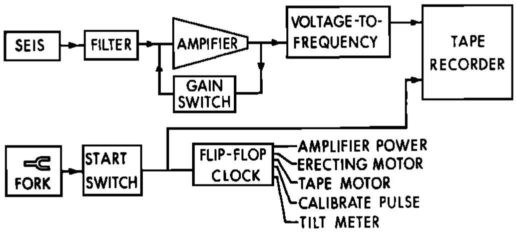

Fig. 1. Block diagram of ocean-bottom single-component vertical seismometer.

and tape recorder after a preset delay and turn it off after 1 hour of recording. A block-diagram of the system is shown in Figure 1. The package was engineered by United ElectroDynamics Corporation. The seismometer has a 1.6-kg moving magnet mass and a 2000-ohm coil, giving 0.7 μv/mμ motion at 1 cps at 0.7 critical damping. The resonant frequency of the instrument is 1 cps. Therefore, the sensitivity of the instrument falls off with decreasing frequency at approximately the same rate at which the microseism noise motion increases, down to the frequency of approximately 1/7 cps. The amplifier is a standard UED solid-state seismic amplifier, with gain up to 10^6. It has a high-frequency, two-stage, cutoff filter at 10 cps and a low-frequency cutoff filter at 0.1 cps. The voltage-to-frequency converter is an I.R.I.G. standard $\pm 40\%$ modulation, for ± 1.36 volts swing. Center frequency is 1.688 kc/s. The over-all dynamic range of the system, including playback, is 40 db. The recorder uses ½-inch magnetic tape at a speed of 1⅞ in./sec. Three tracks are available for recording the seismometer signals. A 582-cps signal from a precision fork is recorded on a fourth track, so that we can compensate for variations in tape speed.

The seismometer can function from vertical to within 20° of horizontal by virtue of a motor-driven screw which adjusts spring tension to center the mass at the start of the recording cycle. The angle and compass orientation of the instrument as it rests on the bottom is recorded by a tilt meter mounted inside the pressure sphere. The tilt indicator is an AG-1 flashbulb in a pendulum, with a fiducial aperture to expose Eastman Photo Resist coating when the bulb fires.

The various functions of the instrument, such as centering the seismometer mass, activating the tilt recorder, turning on the amplifier, initiating the recording cycle, and terminating the recording cycle, are sequenced by an electronic clock. The time base of this clock is the precision tuning fork mentioned earlier. The recording cycle starts 3 hours after the clock is started and terminates 1 hour later. The clock is started on the surface immediately before the instrument is released, and the 3-hour de-

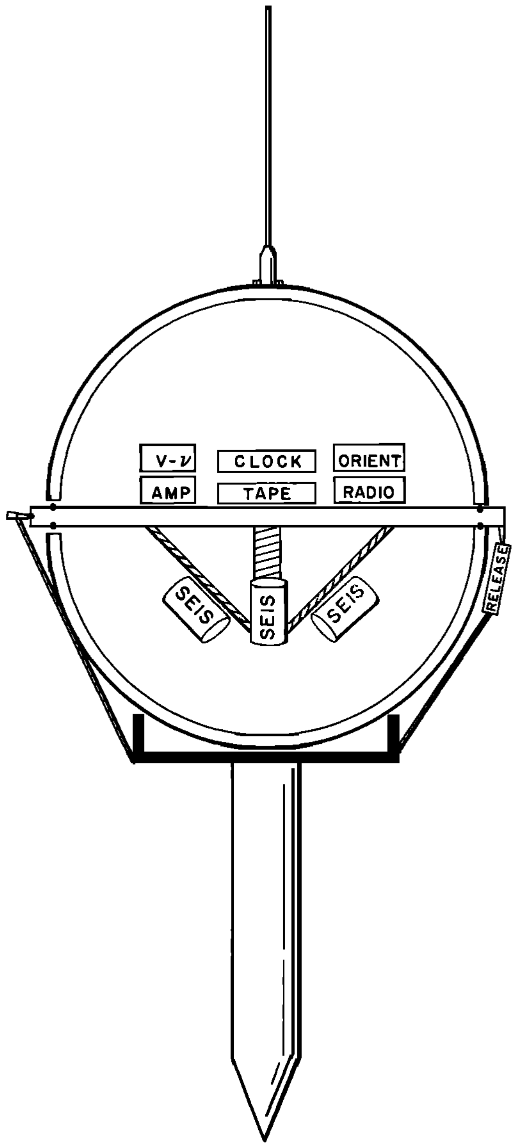

Fig. 2. Schematic of the package assembly. The spherical section will withstand a pressure of greater than 600 bars and has a net buoyancy of approximately 10 kg in sea water. The spike anchor weighs 70 kg.

lay allows adequate time for the instrument to come to rest on the ocean bottom.

Power for all functions is provided by low-temperature mercury batteries. The pressure vessel that contains the seismographic equipment is made from two deep-drawn hemispheres of 7178 T-6 aluminum. The 22-in. ID hemispheres were designed and fabricated by Alcoa, New Kensington, Pennsylvania. The spheres are assembled by clamping, with six angle-brackets, onto an O-ringed aluminum center plate, which carries all the instruments in the sphere. Electrical leads, can be brought out through the aluminum center plate, or through the surface of the sphere, by Mecca plugs or by similar high-pressure bulkhead connectors. A Mecca plug mounted through the top of the hemisphere serves as antenna feed-through for the citizen's band radio recovery beacon. Seal-screws are threaded through the center plate, so that the sphere can be flushed with dry air after assembly, and air can be let into the sphere to permit disassembly after recovery from the cold ocean. Figure 2 shows the package assembly.

The anchor for the seismometer package is a lead spike, 4 in. in diameter, and 20 in. long, with a 30° conical tip. The top of the spike terminates in a dish-shaped flange, 16 in. in diameter, which carries three cable-eyes for attachment to the buoyant seismometer sphere. The dimensions were chosen so that the spike would penetrate 15 to 20 in. into the mud-clay sediment of the San Diego trough which has a bearing strength of 1 to 3 lb/in^2. This rigidity of bottom is said to be characteristic of the broad, flat Pacific Ocean basin. If the anchor strikes soft mud, the flange keeps the package from penetrating into it so far that the anchor release is obstructed. The 15-in. penetration in the San Diego trough was confirmed by observing clay adhering to recovered anchors. The in-

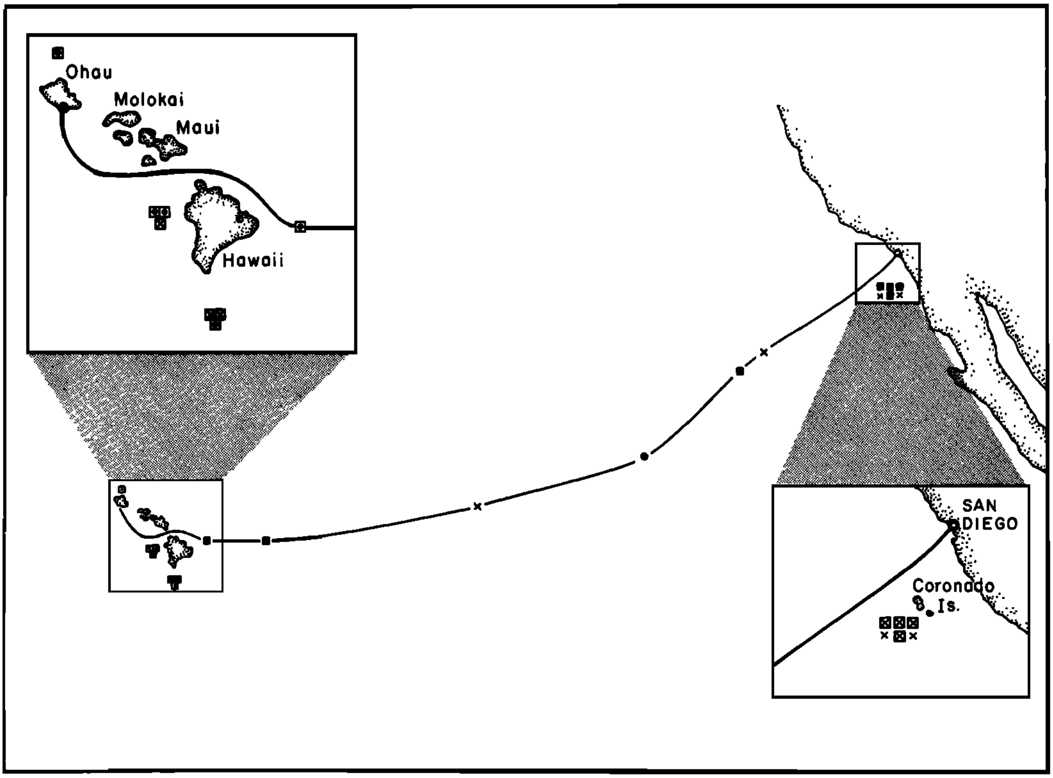

Fig. 3. Approximate locations of ocean-bottom seismic stations. Land stations were occupied on Hawaii, Oahu, and near San Diego.

TABLE 1. Ocean Bottom Stations, Fall and Winter, 1962–1963

Date	Starting Time, (UT) h m	Location	Depth, km	No. of Components	Tilt, deg	Core
1962						
Oct. 14	20 00	19°40′N 156°30′W	4.600	1	17	
Oct. 17	20 00	19°51′N 156°36′W	4.600	1	15	
Oct. 21	20 00	19°45′N 156°36′W	4.600	3	17	
Oct. 22	20 00	17°45′N 156°26′W	4.700	1		
Oct. 23	20 00	17°45′N 156°29′W	4.700	3	22	
Oct. 24	20 00	17°45′N 156°29′N	4.700	3	12	
1963						
Jan. 21	20 00	22°28′N 158°00′W	4.600	1	12	
Feb. 7	21 00	20°16′N 154°13′W	5.400	3	24	Lt brn clay mud
Feb. 8	21 00	19°58′N 151°11′W	5.300	3		Lt brn, very soft
Feb. 12	15 00	22°07′N 139°00′W	5.100	1	16	Brn-medium mud
Feb. 14	19 00	23°12′N 130°58′W	4.850	3	14	Brn clay mud
Feb. 16	15 00	27°30′N 125°46′W	4.400	1		Brn clay mud
Feb. 17	15 00	28°36′N 124°01′W	4.350	1	21	Brn clay mud

strument package separates from the anchor by means of a magnesium release [*Van Dorn*, 1953].

Seismic stations. Data have been gathered on and around the Hawaiian Islands, off the coast of Southern California, and at points between Hawaii and California. The approximate locations of these sites are shown in Figure 3. Pertinent details of the ocean-bottom stations are given in Table 1. Details of the land stations are given in Table 2.

Analysis and results. The data can be analyzed in two ways. An analog display can be obtained by demodulating the signal as it is reproduced from the magnetic tape, passing it through a variable frequency band pass filter, and recording the results on a strip chart. An approximate spectrum can be obtained in this manner. An alternative method is to feed the signal directly from the tape to an electronic counter and then to a digital computer. Spectra have been obtained using this method with a CDC 1604 computer and a computer program written for the analysis of time series. We are currently using BOMM, a program written at La Jolla and Cambridge [*Bullard et al.*, 1964].

The land record for the spectrum shown in Figure 4 was taken on bedrock, in an abandoned water tunnel, 5 km from shore, on the windward

TABLE 2. Land Stations, Fall and Winter, 1962–1963

Date	Starting Time, (UT) h m	Location
1962		
Oct. 14	20 00	Hawaii Volcano Observatory
Oct. 18	20 00	Hawaii Volcano Observatory
Oct. 21	20 00	Hawaii Volcano Observatory
Oct. 22	20 00	Hawaii Volcano Observatory
Oct. 23	20 00	Hawaii Volcano Observatory
Oct. 24	20 00	Hawaii Volcano Observatory
1963		
Jan. 21	20 00	Oahu, Waihole Tunnel
Feb. 7	21 00	Oahu, Waihole Tunnel
Feb. 8	21 00	Oahu, Waihole Tunnel
Feb. 9	21 00	Oahu, Waihole Tunnel
Feb. 16	15 00	La Jolla, California

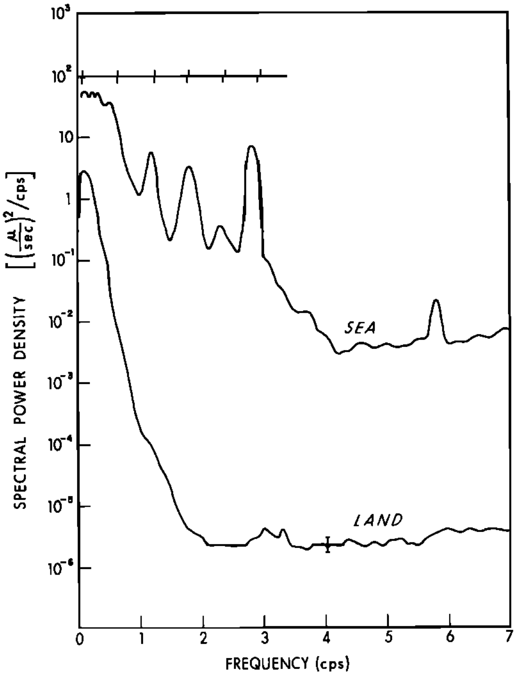

Fig. 4. Seismic background spectra on land and ocean bottom, February 8, 1963, Hawaii. The land instrument was a vertical seismometer. The ocean-bottom instrument contained three-component equiaxial seismometers. Only one component is displayed. The other two components were similar. The scales at the top of the figure show the frequencies of organ-pipe modes in the water. Refer to the text for more details.

side of Oahu in the Hawaiian chain. The ocean-bottom record was taken in 5 km of water approximately 750 km east of the land site. A core sample taken at the site indicated a soft mud bottom. Both records are typical of their respective locations: they were taken at the same time with supposedly identical instruments. No significant coherence between the two records was found. Each spectrum represents a time series 8 minutes long. The Tukey method of spectral analysis was used with 200 lags [*Blackman and Tukey,* 1958]. The sample rate is 18 samples/sec, resulting in 90 degrees of freedom. The transfer functions of the instruments were taken into account during the analysis; therefore the computed spectra represent actual earth noise. Instrument noise is below the minimum signal level for all the spectra shown in this paper. The 60% statistical confidence limit for each ordinate point, separated by 0.05 cps is shown by the vertical bar at 4 cps in Figure 4. Confidence limits for the other spectra of this paper are similar.

The energy of the sea-bottom noise is an order of magnitude higher than that measured on land in the lower frequencies and three or more orders of magnitude higher in the high frequencies. This indicates that a great deal of the microseismic energy we have seen is generated at sea and that the higher frequencies are not transmitted to land. The spectral power density is expressed as $(\mu/\text{sec})^2$ in a 1-cps bandwidth. The power density at 1 cps is 1 $\mu^2\text{sec}^{-1}$ cycle^{-1} for the sea-bottom record, and about 2×10^{-4} μ^2 sec^{-1} cycle^{-1} for the land record. This can be converted to ground velocity per octave by multiplying the energy density by the bandwidth and taking the square root. The conversion gives values of about 800 mμ/sec for the sea-bottom record and about 12 mμ/sec for the land record in the band from 0.7 to 1.4 cps. The power density at the spectral peak is 60 μ^2 sec^{-1} cycle^{-1} for the sea-bottom record and 3 μ^2 sec^{-1} cycle^{-1} for the land record. This corresponds to ground velocity of 2.5 μ/sec and 500 mμ/sec for the sea-bottom and land records, respectively, in the band from 0.1 to 0.2 cps. The peaked structure of the sea-bottom spectrum is characteristic of our sea-bottom records.

The peak power density and general shape of the power spectrum shown in Figure 5 (taken two island diameters from shore) are not significantly different from those for the spectrum of Figure 6 (taken midway between California and Hawaii). Spectral changes with distance from land are much less striking than temporal changes; therefore, we have not been able to infer from these comparisons whether the noise is generated in the ocean near shore, or far from shore.

The ocean-bottom spectra do not always show the pronounced multiple peaks at the same frequencies as can be seen in Figure 7.

Analyses of ocean-bottom three-component seismometer records indicate that only a small proportion of the energy is in the form of Rayleigh waves. More details of the mode distributions will be given in a subsequent paper.

The traces shown in Figure 8 were made by playing back the magnetic tape, passing the signal through a demodulator, and recording

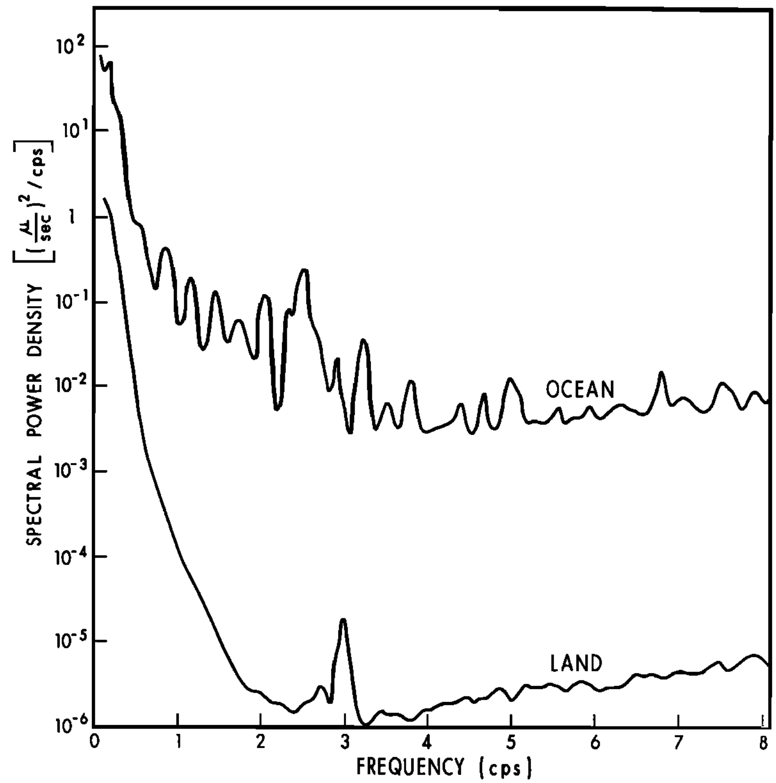

Fig. 5. Seismic background spectra on land and ocean bottom, January 21, 1963, Hawaii. Both instruments were single-component (vertical) seismometers.

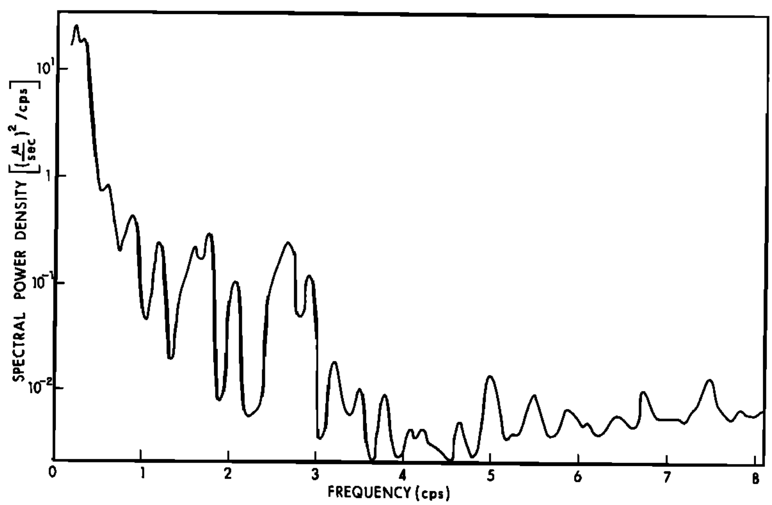

Fig. 6. Seismic background spectrum from single-component instrument on ocean bottom, February 12, 1963.

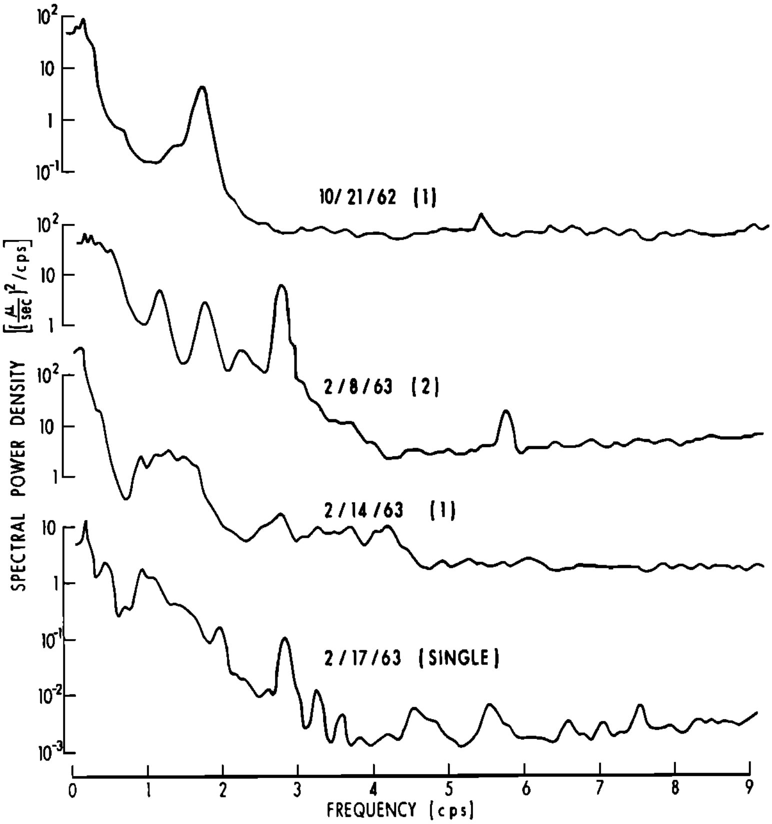

Fig. 7. Comparative spectra from four deep-ocean drops on Pacific floor. The power density for each spectrum is indicated by the segment of scale on the left. The notation on each curve indicates the date and the seismometer (single-component, or one channel of the triaxial seismometer). Details of the stations are given in Table 1.

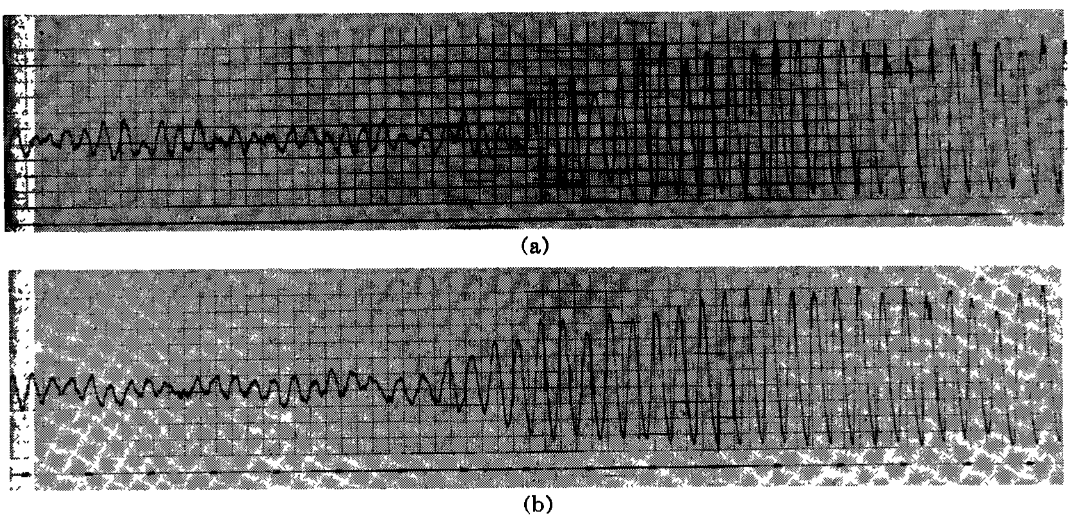

Fig. 8. Analog display of two earthquakes recorded off coast of Hawaii on October 21, 1962. The time marks are 2-sec intervals.

it on a Sanborn strip-chart recorder. A land station located 120 km to the east at the Hawaiian Volcano Observatory did not register the signals, even though the magnification was ten times higher at the land station. These were probably small local shocks on the sea floor which attenuated too rapidly to be seen at the land station.

The timing marks on the lower part of each trace are at 2-sec intervals. The first quake was registered at 20h 21m 10s UT. It had a recorded duration of 90 sec. The second, registered at 20h 30m, had a recorded duration of 380 sec. Unfortunately, we cannot determine any of the details of the shocks because they overloaded the instruments. Since we are primarily interested in the characteristics of the microseismic background noise, rather than seismic signals, we attempt to set the gain of the seismic amplifiers to give maximum output with background noise. The gain settings must be made before the recording, and hence some recordings show very small signals, with a resultant loss of accuracy. Other recordings show large signals, with a resultant distortion which is impossible to analyze. The microseismic noise shown on the left half of Figure 8 represents almost full-scale output of the seismic amplifier. The traces shown on the right half represent the nonlinearities of the seismic amplifier and frequency modulator and the interaction of these signals with the demodulator.

The large amount of high-frequency structure shown in Figure 9 is often seen in our continental land records. The same seismometer was used to obtain the La Jolla and Hawaii land records. Surf conditions during these times were 'normal.' The Hawaii station was approximately 5 km from shore and the La Jolla station was 13 km from shore. If local surf action was responsible for the peaks in the La Jolla records at frequencies between 1 and 8 cps, we would expect that similar high-frequency peaks could be detected on the Hawaii land spectra.

We cannot make such convincing arguments against instrumental resonances in the ocean-bottom seismographs. But the similarity of peak structure between the three-component ocean instrument, the one-component ocean instrument, and the continental land instrument leads us to the tentative conclusion that the peaks are seismic.

The peaked structures of the power spectra may indicate that resonant modes in the layered medium are being excited. The peaks of the February 8 spectrum, Figure 4, correspond very

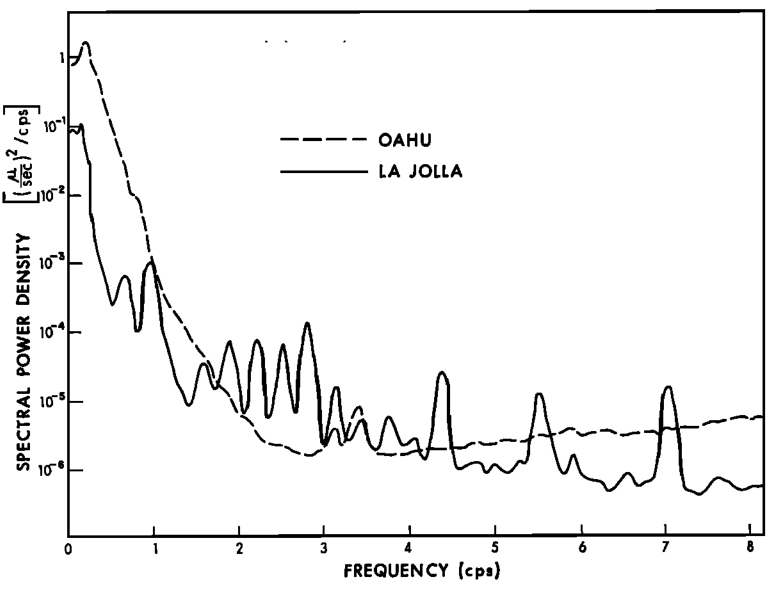

Fig. 9. The seismic background spectra on land. The upper record was obtained on Oahu, Hawaiian Islands, on February 9, 1963. The lower record was obtained near La Jolla, California, on February 16, 1963.

well with excitation of every fourth organ-pipe mode in the water. These modes, with amplitude nodes at the bottom and amplitude antinodes at the top of the water, will have frequencies $\nu_n = (8n + 1)\ C/4D$, where D is water depth and C is the velocity of sound in water. The uppermost scale at the top of Figure 4 shows the frequencies corresponding to the water depth of 5300 meters. The second scale at the top of the figure shows the frequencies corresponding to 5300 meters of water plus 100 meters of mud with the same compressional velocity.

The curves shown in Figure 10 can be considered as transfer functions' from sea bottom to land, if the energy sources lie at sea, beyond the ocean-bottom station, and if the source was stationary from February 16 to February 17, 1963.

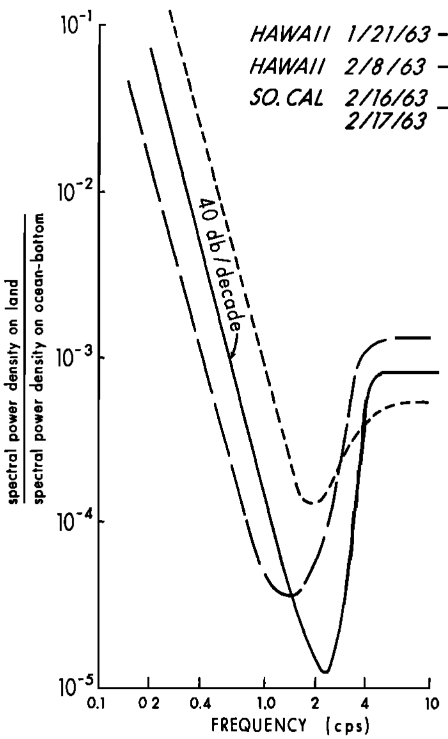

Fig. 10. Smoothed ratios of land spectral power to ocean-bottom spectral power. The curves can be considered as transfer functions from ocean-bottom to land, if the energy sources lie at sea, beyond the ocean-bottom station, and if the source was stationary from February 16 to February 17, 1963.

In conclusion, we find that the ocean bottom appears to be noisier than land, especially at the higher frequencies. Many of the ocean-bottom records show a series of peaks in the power spectrum which might indicate leaky organ-pipe modes. We have not been able to obtain any significant coherences between the ocean-bottom stations and the land stations.

Our spectra appear to be in good agreement with deep-ocean and land seismic backgrounds obtained by the Texas Instrument Company [*Schneider*, 1964]. Some of their earlier records taken on the continental shelf and in shallow water at Catalina Island show lower noise than the deep ocean [*Schneider and Backus*, 1964]. The spectrum levels are, understandably, more like land records. Records made by Lamont Geological Observatory [*Prentiss and Ewing*, 1962; *Ewing*, 1963] show low microseism noise on the deep Atlantic ocean bottom. We do not know why the spectrum levels in the two oceans are so different.

In the future, we plan to study simultaneous records of seismic background, ocean waves, and storms. We hope to extend the dynamic range of our instruments so that we will be able to resolve both background noise and seismic signals. We also plan to add a pressure transducer with a response similar to that of the seismometer to the system. It is hoped that this will give us a means of compensating for the effect of bottom [*Bradner*, 1963].

Ackowledgments. We wish to express appreciation to personnel of the Hawaii Institute of Geophysics, who made all arrangements for the Oahu land station and for ship and crew during operations in Hawaiian waters. In particular, we thank Doak Cox, Martin Vitousek, and Don Cameron for their efforts in checking out equipment and setting up the operation.

We also wish to thank the Hawaii Volcano Observatory, and particularly Harold Krivoy, for making it possible to operate a land station there. The U. S. Navy Fleet Weather Central furnished a full set of weather charts for the period of the Hawaii operation.

Mr. Forrest Whitcomb, of the Institute of Geophysics, University of California, San Diego, designed and built many of the mechanical parts of the system. He was responsible for careful checks during all phases of the operations at sea.

This research was supported by the Air Force Office of Scientific Research under research grant 62-420.

REFERENCES

Blackman, R. B., and J. W. Tukey, *The Measurement of Power Spectra,* Dover Publications, New York, 1958.

Bradner, H., Probing sea-bottom sediments with microseismic noise, *J. Geophys. Res., 68*(6), 1788–1791, 1963.

Bullard, E. C., F. E., Oglebay, W. H. Munk, and G. R. Miller, *A User's Guide to Bomm* (in preparation), University of California, San Diego, 1964.

Donn, W. L., The relationship between microseism period and storm position, *Science, 119,* 55–57, 1954.

Ewing, M., Lamont Geological Observatory Final Report on Contract AF 19(604)8357, August 31, 1963.

Haubrich, R. A., and H. M. Iyer, A digital seismograph system for measuring earth noise, *Bull. Seismol. Soc. Am., 52,* 87–93, 1962.

Haubrich, R. A., W. H. Munk, and F. E. Snodgrass, Comparative spectra of microseism and swell, *Bull. Seismol. Soc. Am., 53,* 27–37, 1963.

Lehner, F. E., Brief description of Ranger lunar seismograph, *Proc. IRE, 50,* 2297, 1962.

Monakhov, F. I., and N. A. Dolbilkina, The structure of microseism, *Izv. Akad. Nauk SSSR, Ser. Geofiz,* 937–945, 1958.

Monakhov, F. I., and N. A. Dolbilkina, The structure of microseisms and methods of determining direction of the source of their origin, *Izv. Akad. Nauk SSSR, Ser. Geofiz,* 1463–1465, 1960.

Prentiss, D. P., and J. I. Ewing, The seismic motion of the deep ocean floor, Lamont Geological Observatory Annual Report, Contract AF 19-(604)8357, 1 April, 1961—31 December 1962.

Schneider, W. A., and M. M. Backus, Ocean-bottom seismic measurements off the California coast, *J. Geophys. Res., 69,* 1135–1143, 1964.

Van Dorn, W. G., The marine release-delay timer, *Scripps Inst. Oceanog. Ref. 53-23,* 1953.

(Manuscript received March 30, 1964;
revised June 5, 1964.)